LHCb-CONF-2019-005
November 13, 2019

Multiplicity-dependent modification of $\chi_{c1}(3872)$ and $\psi(2S)$ production in pp collisions at $\sqrt{s} = 8$ TeV

LHCb collaboration†

Abstract

In pp collisions at $\sqrt{s} = 8$ TeV, $\chi_{c1}(3872)$ and $\psi(2S)$ states are produced promptly at the primary collision vertex or in decays of b hadrons. We study their relative production rates as a function of particle multiplicity. The fraction of promptly produced states is found to decrease with multiplicity for both $\chi_{c1}(3872)$ and $\psi(2S)$. This evolution differs between the two species: the ratio of cross-sections for promptly produced particles, $\sigma_{\chi_{c1}(3872)}/\sigma_{\psi(2S)}$, is found to decrease with increasing multiplicity. By contrast, no significant dependence on multiplicity is observed for the equivalent ratio for $\chi_{c1}(3872)$ and $\psi(2S)$ produced in b-hadron decays. This behaviour is consistent with the interpretation of the $\chi_{c1}(3872)$ as a weakly bound state, such as a $D^0\overline{D}^{*0}$ hadronic molecule.

†Conference report prepared for Quark Matter 2019 - the XXVIIIth International Conference on Ultrarelativistic Nucleus-Nucleus Collisions, Wuhan, China, 3-9 November 2019. Contact author: J. Matthew Durham, durham@lanl.gov

1 Introduction

In recent years, multiple new resonances containing heavy quarks have been observed which do not fit in the framework of conventional hadrons (see Ref. [1] for a recent review). The most studied of these exotic hadrons is the $\chi_{c1}(3872)$, also known as $X(3872)$. It was first discovered in the mass spectrum of $J/\psi\,\pi^+\pi^-$ in B-meson decays at Belle [2], and has since been confirmed in multiple decay channels at other experiments [3–6]. Despite intense experimental and theoretical scrutiny, the exact nature of the $\chi_{c1}(3872)$ meson is still unclear.

Multiple explanations of the $\chi_{c1}(3872)$ structure have been proposed. Shortly after its discovery, it was considered as one of several possible charmonium states [7]. However, LHCb measurements have since confirmed the quantum numbers to be $J^{PC} = 1^{++}$ [8], which disfavors assignment as conventional charmonium because no compatible charmonium states are expected to exist near the measured mass [9]. Other models consider the $\chi_{c1}(3872)$ state to be a tetraquark, which may have further substructure composed of a diquark-antidiquark bound state [10–12], or a hadrocharmonium state where two light quarks orbit a charmonium core [13]. Mixtures of various exotic and conventional states have also been studied [14–16].

The remarkable proximity of the $\chi_{c1}(3872)$ mass and the sum of the D^0 and $\overline{D}^{*0}$ meson masses led to the consideration of its structure as a hadronic molecule, a state consisting of these two mesons bound via pion exchange [17, 18]. In this case, the binding energy of the $\chi_{c1}(3872)$ hadron would be small, as the mass defect, defined as $M_{\chi_{c1}(3872)} - (M_{D^0} + M_{\overline{D}^{*0}}) = 0.01 \pm 0.27\,\mathrm{MeV}/c^2$, is consistent with zero. Consequently, these models attribute the $\chi_{c1}(3872)$ a large radius, of order 7 fm [16, 19].

Weakly bound quarkonium states have been studied extensively in proton-nucleus and nucleus-nucleus collisions. Measurements of charmonium production in pA collisions at fixed target experiments [20, 21] and colliders [22–26] showed that the $\psi(2S)$ is suppressed more than the J/ψ in rapidity regions where a relatively large number of charged particles are produced. Similarly, measurements of Υ production at the Large Hadron Collider (LHC) revealed that the $\Upsilon(2S)$ and $\Upsilon(3S)$ states are suppressed more than the $\Upsilon(1S)$ [27, 28]. As the effects governing heavy quark production and transport through the nucleus are similar for states with the same quark content, the mechanism for the suppression of excited states is expected to occur in the late stages of the collision, after the $Q\bar{Q}$ pair has hadronized into a final state. Models incorporating final state effects, such as breakup via interactions with co-moving hadrons, are able to describe the relative suppression of excited quarkonium states in pA collisions [29–32]. If the $\chi_{c1}(3872)$ is a hadronic molecule with a small binding energy and large radius, similar final-state effects could also disrupt its formation, via interactions with pions produced in the underlying event [33].

High-multiplicity pp collisions provide a hadronic environment that approaches heavy ion collisions in many respects. Recently, phenomena typically thought only to occur in collisions of large nuclei have been observed in high multiplicity pp collisions, including a near-side ridge in two-particle angular correlations [34], strangeness enhancement [35], and collective flow [36]. Therefore, it is possible that high-multiplicity pp collisions provide a testing ground for examining final-state effects observed on quarkonia in pA collisions.

In this Note, we present measurements of the fractions of $\chi_{c1}(3872)$ and $\psi(2S)$ states that are produced promptly (directly at the pp collision vertex), f_{prompt}, in pp collisions as a function of the event activity. The $\chi_{c1}(3872)$ and $\psi(2S)$ candidates are reconstructed through their decays to $J/\psi\,(\rightarrow \mu^+\mu^-)\pi^+\pi^-$. The study uses a sample of data collected with the LHCb detector at a center-of-mass energy $\sqrt{s} = 8\,\mathrm{TeV}$, corresponding to an integrated luminosity of $2\,\mathrm{fb}^{-1}$. To enable a direct comparison between the exotic $\chi_{c1}(3872)$ state and the conventional charmonium state $\psi(2S)$, we also report the ratio of the $\chi_{c1}(3872)$ to $\psi(2S)$ cross sections, as a function of event activity, for prompt production at the collision vertex and production in decays of b hadrons. In this analysis, the event activity is represented by the number of charged particle tracks reconstructed in the silicon strip detector located around the pp collision region.

2 Detector and simulation

The LHCb detector [37, 38] is a single-arm forward spectrometer covering the pseudorapidity range $2 < \eta < 5$, designed for the study of particles containing b or c quarks. The detector includes a high-precision tracking system consisting of a silicon-strip vertex detector surrounding the pp collision region (VELO), a large-area silicon-strip detector located upstream of a dipole magnet with a bending power of about $4\,\mathrm{Tm}$, and three stations of silicon-strip detectors and straw drift tubes placed downstream of the magnet. The tracking system provides a measurement of the momentum, p, of charged particles with a relative uncertainty that varies from 0.5% at low momentum to 1.0% at $200\,\mathrm{GeV}/c$. The minimum distance of a track to a primary collision vertex (PV), the impact parameter (IP), is measured with a resolution of $(15 + 29/p_\mathrm{T})\,\mu\mathrm{m}$, where p_T is the component of the momentum transverse to the beam, in GeV/c. Different types of charged hadrons are distinguished using information from two ring-imaging Cherenkov (RICH) detectors. Photons, electrons and hadrons are identified by a calorimeter system consisting of scintillating-pad and preshower detectors, an electromagnetic and a hadronic calorimeter. Muons are identified by a system composed of alternating layers of iron and multiwire proportional chambers. The online event selection is performed by a trigger, which consists of a hardware stage, based on information from the calorimeter and muon systems, followed by a software stage, which applies a full event reconstruction.

Simulation is required to model the effects of the detector acceptance and the imposed selection requirements. In the simulation, pp collisions are generated using Pythia [39,40] with a specific LHCb configuration [41]. Decays of unstable particles are described by EvtGen [42]. The interaction of the generated particles with the detector, and its response, are implemented using the Geant4 toolkit [43] as described in Ref. [44].

3 Data analysis

Events considered in this analysis are selected by a set of triggers designed to record events containing the decay $J/\psi \rightarrow \mu^+\mu^-$. The first stage is a hardware trigger, which requires at least one track passing through all five stations of the muon detector that comes from the primary collision vertex. Events selected by this trigger are then passed to the high-level trigger in software, which requires two tracks reconstructed in the muon detector, each having total momentum $p > 6$ GeV/c and transverse momentum $p_\mathrm{T} > 500$ MeV/c. The two muon candidates form a pair with an invariant mass above 2.7 GeV/c^2.

Tracks from triggered events which produce hits in all five muon detector stations are selected as muon candidates in the present analysis. They are required to have total momentum $p > 10$ GeV/c and transverse momentum $p_{\mathrm{T}} > 650$ MeV/c. The J/ψ peak in the $\mu^+\mu^-$ invariant-mass spectrum is fit, and dimuon combinations which fall within three standard deviations of the mean value and have $p_{\mathrm{T}} > 3$ GeV/c are retained as J/ψ candidates. Charged pion candidates are selected using particle identification information from the RICH detectors. These tracks are required to have $p > 3$ GeV/c, in order to provide maximum pion identification efficiency, and have $p_{\mathrm{T}} > 500$ MeV/c to reduce combinatorial background. Two muon and two pion tracks forming a good-quality common vertex are refit and are retained as $\chi_{c1}(3872)$ and $\psi(2S)$ candidates. The refitting includes kinematic constraints that require all particles to originate from a common vertex and constrains the dimuon mass to the known J/ψ mass [45]. The decay kinematics are required to satisfy constraints on the reaction Q value of $M_{J/\psi\pi^+\pi^-} - M_{J/\psi} - M_{\pi^+\pi^-} < 300$ MeV/c^2, and the candidates must have $p_{\mathrm{T}} > 5$ GeV/c and be within the pseudorapidity range $2 < \eta < 4.5$.

In this analysis the event activity is represented by the total number of charged particle tracks reconstructed in the VELO detector, $N^{\mathrm{VELO}}_{\mathrm{tracks}}$, which is proportional to the total charged particle multiplicity produced in the event. To avoid biases from tracks produced in multiple collisions that occur during a single beam crossing, only events with a single reconstructed PV are considered. The position of collision vertices is constrained to a range where the acceptance is stable, -60 mm $< z <$ 120 mm, to avoid biases from missing tracks that fall outside the VELO. For the reconstructed tracks considered in this analysis, the VELO track reconstruction efficiency has been measured to be constant at $\sim$99% [46]. The resulting $J/\psi\pi^+\pi^-$ invariant-mass spectrum is shown in Fig. 1.

Both $\chi_{c1}(3872)$ and $\psi(2S)$ hadrons can be produced promptly in the pp collision vertex or in the decays of b hadrons, which travel several mm before decaying. The prompt component of the signal is separated from the component originating from b decays by performing a simultaneous fit of the $J/\psi\pi^+\pi^-$ invariant-mass spectrum and the pseudo proper-time spectrum. The pseudo proper-time t_z is defined as

$$t_z = \frac{(z_{\mathrm{decay}} - z_{\mathrm{PV}})M}{p_z}, \tag{1}$$

where $z_{\mathrm{decay}} - z_{\mathrm{PV}}$ is the difference between the positions of the reconstructed vertex of the $J/\psi\pi^+\pi^-$ and the collision vertex along the beam axis, M is the known mass [45] of the reconstructed hadron, and p_z is the candidate's momentum along the beam axis. The proper-time spectrum is fit with a delta function representing the prompt component and an exponential decay function representing the component from b decays, which are convolved with a double Gaussian resolution function, plus a background component. Two different parametrizations of the background component are used. The first uses an empirically determined function, as was done in Ref. [47]. The other method uses the t_z shape obtained from mass sidebands above and below the mass peak of interest. The fits return the fraction of the inclusive signal that is produced at the collision vertex, f_{prompt}. The central value of f_{prompt} is taken as the average of the values obtained using these two methods, while the difference is taken as a systematic uncertainty, which is typically 1% to 2% for the $\psi(2S)$ fits, and ranges from 2% to 8% for the $\chi_{c1}(3872)$ fits.

In the fit to the invariant-mass spectrum, the $\psi(2S)$ peak is represented by a sum of two Crystal Ball functions, as in a previous LHCb analysis at 7 TeV [48]. The $\chi_{c1}(3872)$ line shape, which is dominated by detector resolution effects due to its narrow natural width, is well described by a Gaussian. The background contribution is studied by examining the invariant-mass spectrum constructed by using pion pairs with the same charge, and is found to be well described by a third order Chebychev polynomial; this shape is used to represent the background when fitting the $J/\psi\,\pi^+\pi^-$ mass spectra. The invariant mass and t_z spectra are divided into bins of $N^{\rm VELO}_{\rm tracks}$, and the fit is performed in each bin. Example fit projections to the $\psi(2S)$ mass and t_z spectra for the range $60 < N^{\rm VELO}_{\rm tracks} < 80$ are shown in Fig. 2.

We examine the prompt and b-decay components directly by calculating the ratio of cross sections, $\sigma_{\chi_{c1}(3872)}/\sigma_{\psi(2S)}$, times their decay branching fractions to $J/\psi\,\pi^+\pi^-$

$$\frac{\sigma_{\chi_{c1}(3872)}}{\sigma_{\psi(2S)}}\frac{\mathcal{B}[\chi_{c1}(3872)\to J/\psi\,\pi^+\pi^-]}{\mathcal{B}[\psi(2S)\to J/\psi\,\pi^+\pi^-]} = \frac{N_{\chi_{c1}(3872)}\,f^{\chi_{c1}(3872)}_{\rm prompt}}{N_{\psi(2S)}\,f^{\psi(2S)}_{\rm prompt}}\,\frac{\varepsilon_{\psi(2S)}}{\varepsilon_{\chi_{c1}(3872)}}. \tag{2}$$

In Eq. (2) N_R is the signal yield, $f^R_{\rm prompt}$ is the prompt fraction of $R = \psi(2S), \chi_{c1}(3872)$ determined in the simultaneous fit to the $J/\psi\,\pi^-\pi^+$ invariant-mass spectrum and proper-time distribution, and ε_R is the signal efficiency. The overall signal efficiency may be expressed as

$$\varepsilon_R = \varepsilon^{\rm acc}_R\,\varepsilon^{\rm reco}_R\,\varepsilon^{{\rm PID}\mu}_R\,\varepsilon^{{\rm PID}\pi}_R, \tag{3}$$

where $\varepsilon^{\rm acc}_R$ is the efficiency for the state R and its four charged decay products to fall within the LHCb acceptance, $\varepsilon^{\rm reco}_R$ is the efficiency for trigger, reconstruction, and selection

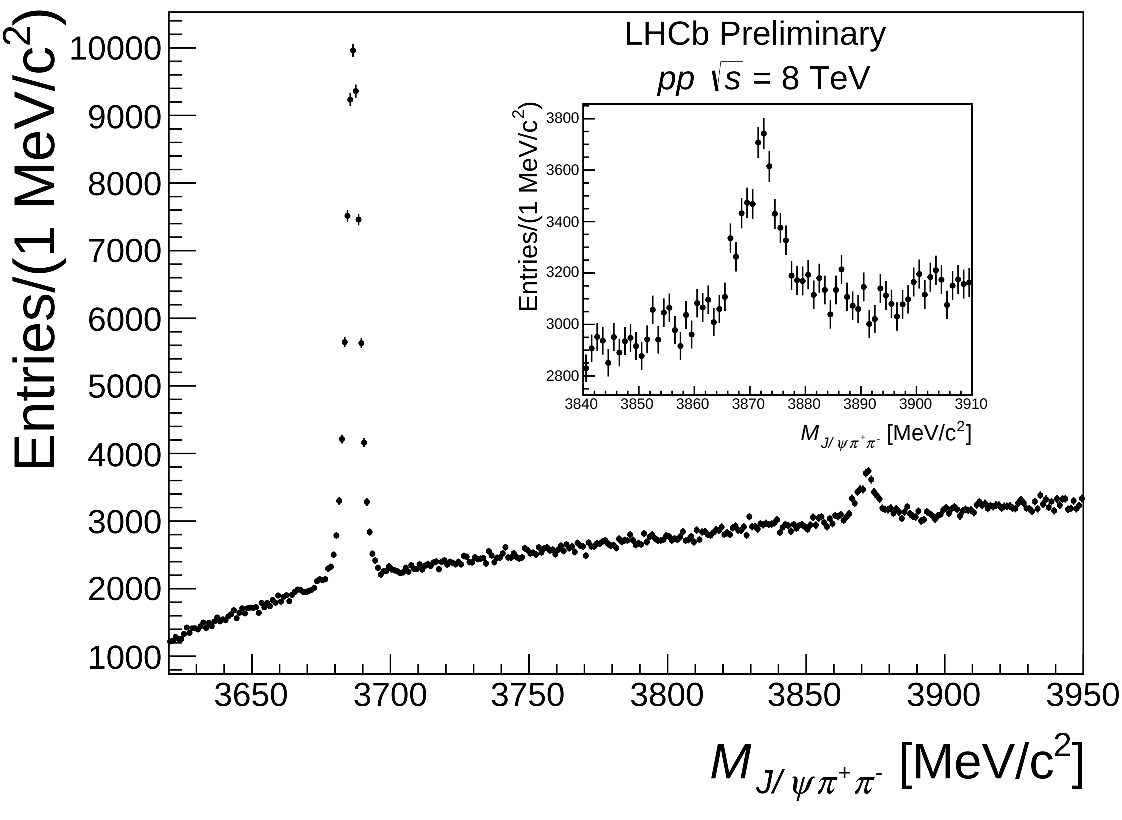

Figure 1: The $J/\psi\,\pi^+\pi^-$ invariant-mass spectrum. The insert shows the region of the $\chi_{c1}(3872)$ resonance.

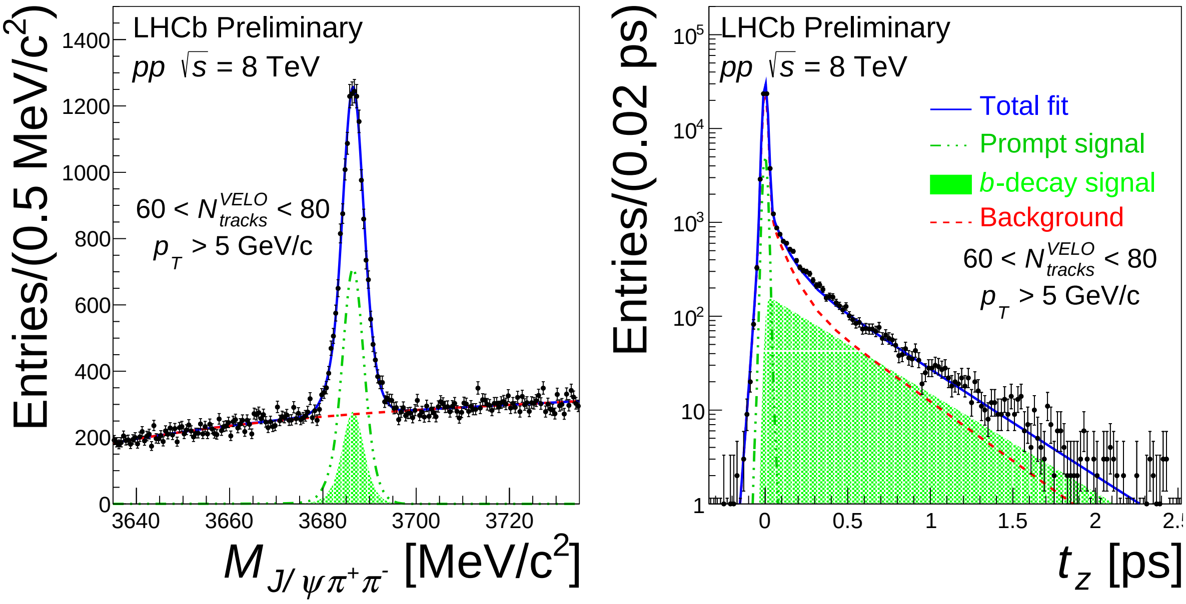

Figure 2: Simultaneous fits to the mass (left) and pseudo proper-time t_z (right) of the $\psi(2S)$, in the event activity range $60 < N_{\text{tracks}}^{\text{VELO}} < 80$. The data is shown as black points and the total fit is shown as a blue line. The fit components consist of background (red dashed line), the prompt signal component (green dashed line), and the b-decay signal component (shaded green).

of the signal candidate, and $\varepsilon_R^{\text{PID}\mu}$ and $\varepsilon_R^{\text{PID}\pi}$ are data-driven corrections for the particle identification efficiency of muons and pions. The acceptance and reconstruction efficiencies are determined from Monte Carlo simulation, followed by data-driven corrections to the tracking and PID selection efficiency obtained with control samples of data. Over the range of $N_{\text{tracks}}^{\text{VELO}}$ considered here, the track reconstruction efficiency varies by $\sim$1%, and is well described by simulation [49]. The efficiency ratio, $\varepsilon_{\psi(2S)}/\varepsilon_{\chi_{c1}(3872)}$, is found to be 0.61, significantly different from unity; this is primarily due to differences in $\varepsilon^{\text{reco}}$ between the two decay processes: $\varepsilon_{\psi(2S)}^{\text{reco}}/\varepsilon_{\chi_{c1}(3872)}^{\text{reco}} = 0.62$. The remaining corrections, given below, are close to unity.

Systematic uncertainties are assigned for each element of the efficiency correction. The uncertainty on $\varepsilon_{\psi(2S)}^{\text{reco}}/\varepsilon_{\chi_{c1}(3872)}^{\text{reco}}$ is the dominant systematic uncertainty on the measured cross section ratio, and is governed by the lack of data on $\chi_{c1}(3872)$ distributions. First, the mean efficiency depends on the kinematic distribution of the signal, which may differ between simulation and data. To assess the dependence of the result on the assumed distribution, the simulated candidates are reweighted based on previous experimental measurements and the efficiency recomputed. LHCb has measured the p_{T} and rapidity distributions of $\psi(2S)$ mesons at $\sqrt{s} = 7$ and 13 TeV, and the $\psi(2S)$ signal in this analysis is weighted to reproduce these (first for 7 TeV and then for 13 TeV). No equivalent measurements are available for $\chi_{c1}(3872)$ hadrons, so the $\psi(2S)$ distributions are used with m_{T} scaling applied, that is, the substitution $p_{\text{T}} \to m_{\text{T}} = \sqrt{p_{\text{T}}^2 + (M_{\chi_{c1}(3872)}^2 - M_{\psi(2S)}^2)}$ from Hagedorn's statistical thermodynamics model of particle production [50]. The efficiency ratio is then recomputed, for 7 TeV and for 13 TeV input. As an additional check,

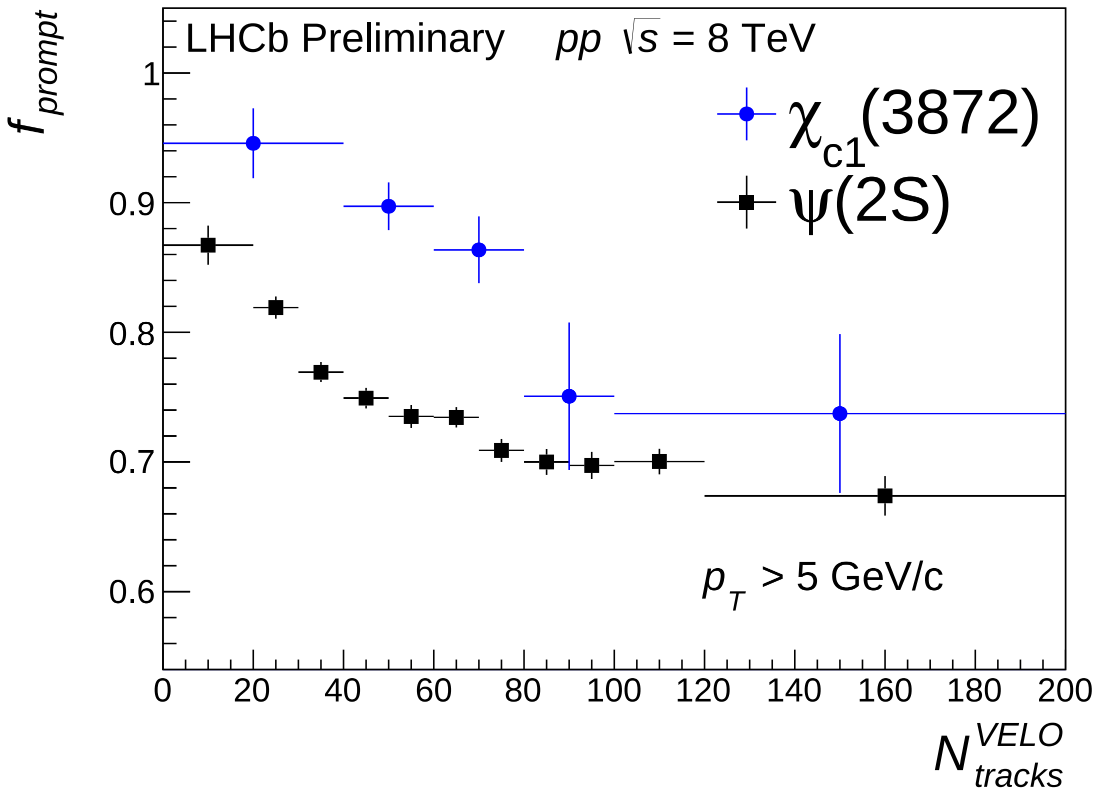

Figure 3: The fraction f_{prompt} of promptly produced $\chi_{c1}(3872)$ and $\psi(2S)$ hadrons, as a function of the number of tracks reconstructed in the VELO.

the kinematic distribution of $\chi_{c1}(3872)$ is reweighted to be identical to that of $\psi(2S)$ mesons. The largest change seen, associated with the final check, is assigned as a systematic uncertainty, leading to $\varepsilon^{\text{acc}}_{\psi(2S)}/\varepsilon^{\text{acc}}_{\chi_{c1}(3872)} = 1.03 \pm 0.02$ and $\varepsilon^{\text{reco}}_{\psi(2S)}/\varepsilon^{\text{reco}}_{\chi_{c1}(3872)} = 0.62 \pm 0.17$. Second, the finite size of the control samples used for the data-driven corrections leads to the corresponding uncertainties: $\varepsilon_R^{\text{PID}\mu} = 0.96 \pm 0.02$ and $\varepsilon_R^{\text{PID}\pi} = 1.00 \pm 0.02$.

4 Results

The prompt fraction f_{prompt} is shown as a function of $N^{\text{VELO}}_{\text{tracks}}$ in Fig. 3. We see a clear decrease as the event activity increases, for both $\psi(2S)$ and $\chi_{c1}(3872)$ hadrons, which could be due to a combination of several effects. The average multiplicity of events where a pair of b quarks is produced is larger than events where they are not produced, due to their fragmentation into hadrons and subsequent decays [51, 52]. This naturally leads to a larger b-decay component in events with high multiplicity. Another effect that could occur is the suppression of prompt $\psi(2S)$ and $\chi_{c1}(3872)$ production via interactions with other particles produced at the vertex, which decreases prompt production in high multiplicity events, but does not affect production in b decays.

To examine these effects, we separately consider the ratio of cross sections $\sigma_{\chi_{c1}(3872)}/\sigma_{\psi(2S)}$ for prompt and b-decay production, as shown in Fig. 4, where the box

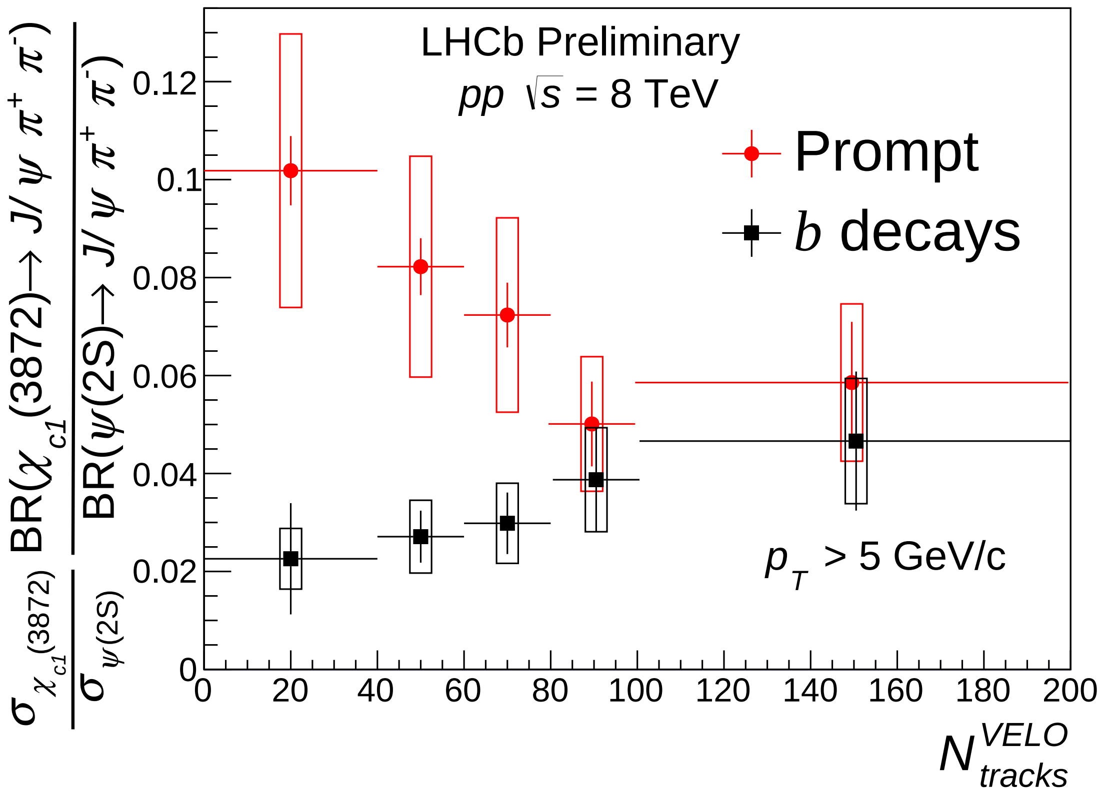

Figure 4: The ratio of the $\chi_{c1}(3872)$ and $\psi(2S)$ cross sections measured in the $J/\psi\pi^+\pi^-$ channel as a function of the number of tracks reconstructed in the VELO.

represents the dominant systematic uncertainty due to the efficiency correction. Moving from low to high multiplicity, prompt $\chi_{c1}(3872)$ production is suppressed relative to prompt $\psi(2S)$ production. This would be expected in a scenario where interactions with co-moving hadrons produced in the collision dissociate the large, weakly bound $\chi_{c1}(3872)$ state more than the relatively compact conventional charmonium state $\psi(2S)$. Fitting a straight line to these data points, without considering the dominant correlated systematic uncertainty shown by the box, yields a slope that is differs from zero by 2.6σ.

In contrast, the ratio of cross sections for production in b decays does not display any significant dependence on event activity, within uncertainties. A straight line fit to these data points, again without considering the correlated systematic uncertainty, gives a slope that is consistent with zero within 1.4σ. This is expected, as these originate from decays of b hadrons in vacuum, and are not subject to any interaction with other particles produced in the event. As such this ratio is set only by the branching fractions of b decays to $\chi_{c1}(3872)$ and $\psi(2S)$ hadrons. This also serves as an important cross check which shows that the observed modification of the prompt component is not the result of detector effects.

5 Summary

In conclusion, we have measured that the prompt $\chi_{c1}(3872)$ and prompt $\psi(2S)$ production cross sections decrease relative to production via b decays as charged particle multiplicity increases in pp collisions at 8 TeV. A direct comparison between the exotic state $\chi_{c1}(3872)$ and the conventional charmonium state $\psi(2S)$ shows that prompt production of $\chi_{c1}(3872)$ may be suppressed relative to prompt $\psi(2S)$ production as multiplicity increases, which could indicate that $\chi_{c1}(3872)$ hadrons are being dissociated via interactions with co-moving particles at the vertex. The b-decay component, which is produced away from the other hadrons in the event, displays no significant dependence on event activity as expected. These results are consistent with the interpretation of the $\chi_{c1}(3872)$ as a weakly bound state, such as a $D^0\overline{D}^{*0}$ hadronic molecule.

References

[1] S. L. Olsen, T. Skwarnicki, and D. Zieminska, *Nonstandard heavy mesons and baryons: experimental evidence*, Rev. Mod. Phys. **90** (2018) 015003.

[2] Belle collaboration, S.-K. Choi *et al.*, *Observation of a narrow charmoniumlike state in exclusive* $B^{\pm} \to K^{\pm}\pi^{+}\pi^{-}J/\psi$ *decays*, Phys. Rev. Lett. **91** (2003) 262001.

[3] CDF II collaboration, D. Acosta *et al.*, *Observation of the narrow state* $X(3872) \to J/\psi\pi^{+}\pi^{-}$ *in* $p\overline{p}$ *collisions at* $\sqrt{s} = 1.96$ TeV, Phys. Rev. Lett. **93** (2004) 072001.

[4] D0 collaboration, V. M. Abazov *et al.*, *Observation and properties of the* $X(3872)$ *decaying to* $J/\psi\pi^{+}\pi^{-}$ *in* $p\overline{p}$ *collisions at* $\sqrt{s} = 1.96$ TeV, Phys. Rev. Lett. **93** (2004) 162002.

[5] BABAR collaboration, B. Aubert *et al.*, *Study of the* $B^{-} \to J/\psi K^{-}\pi^{+}\pi^{-}$ *decay and measurement of the* $B^{-} \to X(3872)K^{-}$ *branching fraction*, Phys. Rev. D **71** (2005) 071103.

[6] LHCb collaboration, R. Aaij *et al.*, *Observation of* $X(3872)$ *production in pp collisions at* $\sqrt{s} = 7$ *TeV*, Eur. Phys. J. **C72** (2012) 1972, `arXiv:1112.5310`.

[7] E. J. Eichten, K. Lane, and C. Quigg, *Charmonium levels near threshold and the narrow state* $X(3872) \to \pi^{+}\pi^{-}J/\psi$, Phys. Rev. D **69** (2004) 094019.

[8] LHCb collaboration, R. Aaij *et al.*, *Determination of the* $X(3872)$ *meson quantum numbers*, Phys. Rev. Lett. **110** (2013) 222001, `arXiv:1302.6269`.

[9] T. Barnes, S. Godfrey, and E. S. Swanson, *Higher charmonia*, Phys. Rev. D **72** (2005) 054026.

[10] L. Maiani, F. Piccinini, A. D. Polosa, and V. Riquer, *Diquark-antidiquark states with hidden or open charm and the nature of* $X(3872)$, Phys. Rev. D **71** (2005) 014028.

[11] R. D. Matheus, S. Narison, M. Nielsen, and J.-M. Richard, *Can the* $X(3872)$ *be a* 1^{++} *four-quark state?*, Phys. Rev. D **75** (2007) 014005.

[12] S. Dubnicka, A. Z. Dubnickova, M. A. Ivanov, and J. G. Körner, *Quark model description of the tetraquark state* $X(3872)$ *in a relativistic constituent quark model with infrared confinement*, Phys. Rev. D **81** (2010) 114007.

[13] P. C. Wallbott, G. Eichmann, and C. S. Fischer, $X(3872)$ *as a four-quark state in a Dyson-Schwinger/Bethe-Salpeter approach*, Phys. Rev. D **100** (2019) 014033.

[14] R. D. Matheus, F. S. Navarra, M. Nielsen, and C. M. Zanetti, *QCD sum rules for the* $X(3872)$ *as a mixed molecule-charmonium state*, Phys. Rev. D **80** (2009) 056002.

[15] M. Butenschoen, Z.-G. He, and B. A. Kniehl, *Deciphering the* $X(3872)$ *via its polarization in prompt production at the CERN LHC*, Phys. Rev. Lett. **123** (2019) 032001.

[16] S. Coito, G. Rupp, and E. van Beveren, *X(3872) is not a true molecule*, Eur. Phys. J. C **73** (2013) 2351.

[17] N. A. Tornqvist, *Isospin breaking of the narrow charmonium state of Belle at 3872-MeV as a deuson*, Phys. Lett. **B590** (2004) 209, arXiv:hep-ph/0402237.

[18] E. Braaten and M. Kusunoki, *Exclusive production of the* $X(3872)$ *in B meson decay*, Phys. Rev. D **71** (2005) 074005.

[19] M. Cardoso, G. Rupp, and E. van Beveren, *Unquenched quark-model calculation of* $X(3872)$ *electromagnetic decays*, Eur. Phys. J. C **75** (2015) 26.

[20] FNAL E866/NuSea collaboration, M. J. Leitch *et al.*, *Measurement of differences between* J/ψ *and* ψ' *suppression in* $p-A$ *collisions*, Phys. Rev. Lett. **84** (2000) 3256.

[21] B. Alessandro *et al.*, J/ψ *and* ψ' *production and their normal nuclear absorption in proton-nucleus collisions at 400 GeV*, Eur. Phys. J. C **48** (2006) 329.

[22] PHENIX collaboration, A. Adare, C. Aidala *et al.*, *Nuclear modification of* ψ', χ_c, *and* J/ψ *production in* $d+\mathrm{Au}$ *collisions at* $\sqrt{s_{NN}} = 200$ GeV, Phys. Rev. Lett. **111** (2013) 202301.

[23] B. Abelev, *Suppression of* ψ*(2S) production in p-Pb collisions at* $\sqrt{s_{NN}}$ *5.02 TeV*, JHEP **2014** (2014) 1.

[24] LHCb collaboration, R. Aaij *et al.*, *Study of* $\psi(2S)$ *production cross-sections and cold nuclear matter effects in pPb collisions at* $\sqrt{s_{NN}}$ *=5 TeV*, JHEP **03** (2016) 133, arXiv:1601.07878.

[25] PHENIX collaboration, A. Adare *et al.*, *Measurement of the relative yields of* $\psi(2S)$ *to* $\psi(1S)$ *mesons produced at forward and backward rapidity in p+p, p+Al, p+Au, and* ^{3}*He+Au collisions at* $\sqrt{s_{NN}} = 200$ *GeV*, Phys. Rev. **C95** (2017) 034904, arXiv:1609.06550.

[26] CMS collaboration, A. M. Sirunyan *et al.*, *Measurement of prompt* ψ*(2S) production cross sections in proton-lead and proton-proton collisions at* $\sqrt{s_{\mathrm{NN}}} =$ *5.02 TeV*, Phys. Lett. **B790** (2019) 509, arXiv:1805.02248.

[27] CMS collaboration, S. Chatrchyan *et al.*, *Event activity dependence of Y(nS) production in $\sqrt{s_{NN}}$=5.02 TeV pPb and $\sqrt{s}$=2.76 TeV pp collisions*, JHEP **04** (2014) 103, `arXiv:1312.6300`.

[28] LHCb collaboration, R. Aaij *et al.*, *Study of Υ production in pPb collisions at $\sqrt{s_{NN}}$ =8.16 TeV*, JHEP **11** (2018) 194, `arXiv:1810.07655`.

[29] A. Capella, A. Kaidalov, A. K. Akil, and C. Gerschel, *J/ψ and ψ' suppression in heavy ion collisions*, Phys. Lett. B **393** (1997) 431.

[30] E. G. Ferreiro, *Excited charmonium suppression in proton-nucleus collisions as a consequence of comovers*, Phys. Lett. B **749** (2015) 98.

[31] Y.-Q. Ma, R. Venugopalan, K. Watanabe, and H.-F. Zhang, *$\psi(2S)$ versus J/ψ suppression in proton-nucleus collisions from factorization violating soft color exchanges*, Phys. Rev. C **97** (2018) 014909.

[32] E. G. Ferreiro and J. P. Lansberg, *Is bottomonium suppression in proton-nucleus and nucleus-nucleus collisions at LHC energies due to the same effects?*, JHEP **2018** (2018) 94.

[33] E. Braaten, H.-W. Hammer, and T. Mehen, *Scattering of an ultrasoft pion and the X(3872)*, Phys. Rev. **D82** (2010) 034018, `arXiv:1005.1688`.

[34] CMS collaboration, V. Khachatryan *et al.*, *Observation of long-range near-side angular correlations in proton-proton collisions at the LHC*, JHEP **09** (2010) 091, `arXiv:1009.4122`.

[35] ALICE collaboration, J. Adam *et al.*, *Enhanced production of multi-strange hadrons in high-multiplicity proton-proton collisions*, Nature Phys. **13** (2017) 535, `arXiv:1606.07424`.

[36] CMS collaboration, V. Khachatryan *et al.*, *Evidence for collectivity in pp collisions at the LHC*, Phys. Lett. **B765** (2017) 193, `arXiv:1606.06198`.

[37] LHCb collaboration, A. A. Alves Jr. *et al.*, *The LHCb detector at the LHC*, JINST **3** (2008) S08005.

[38] LHCb collaboration, R. Aaij *et al.*, *LHCb detector performance*, Int. J. Mod. Phys. **A30** (2015) 1530022, `arXiv:1412.6352`.

[39] T. Sjöstrand, S. Mrenna, and P. Skands, *A brief introduction to PYTHIA 8.1*, Comput. Phys. Commun. **178** (2008) 852, `arXiv:0710.3820`.

[40] T. Sjöstrand, S. Mrenna, and P. Skands, *PYTHIA 6.4 physics and manual*, JHEP **05** (2006) 026, `arXiv:hep-ph/0603175`.

[41] I. Belyaev *et al.*, *Handling of the generation of primary events in Gauss, the LHCb simulation framework*, J. Phys. Conf. Ser. **331** (2011) 032047.

[42] D. J. Lange, *The EvtGen particle decay simulation package*, Nucl. Instrum. Meth. **A462** (2001) 152.

[43] Geant4 collaboration, J. Allison *et al.*, *Geant4 developments and applications*, IEEE Trans. Nucl. Sci. **53** (2006) 270; Geant4 collaboration, S. Agostinelli *et al.*, *Geant4: A simulation toolkit*, Nucl. Instrum. Meth. **A506** (2003) 250.

[44] M. Clemencic *et al.*, *The LHCb simulation application, Gauss: Design, evolution and experience*, J. Phys. Conf. Ser. **331** (2011) 032023.

[45] Particle Data Group, M. Tanabashi *et al.*, *Review of particle physics*, Phys. Rev. **D98** (2018) 030001.

[46] R. Aaij *et al.*, *Performance of the LHCb Vertex Locator*, JINST **9** (2014) P09007, `arXiv:1405.7808`.

[47] LHCb collaboration, R. Aaij *et al.*, *Measurement of $\psi(2S)$ production cross-sections in proton-proton collisions at $\sqrt{s}=7$ and 13 TeV*, `arXiv:1908.03099`, submitted to EPJC.

[48] LHCb collaboration, R. Aaij *et al.*, *Measurement of $\psi(2S)$ meson production in pp collisions at $\sqrt{s}=7$ TeV*, Eur. Phys. J. **C72** (2012) 2100, `arXiv:1204.1258`, Erratum submitted to Eur. Phys. J.C.

[49] LHCb collaboration, R. Aaij *et al.*, *Measurement of the track reconstruction efficiency at LHCb*, JINST **10** (2015) P02007, `arXiv:1408.1251`.

[50] R. Hagedorn, *Statistical thermodynamics of strong interactions at high-energies*, Nuovo Cim. Suppl. **3** (1965) 147.

[51] P. C. Rowson *et al.*, *Charged multiplicity of hadronic events containing heavy quark jets*, Phys. Rev. Lett. **54** (1985) 2580.

[52] OPAL collaboration, G. Abbiendi *et al.*, *Charged particle multiplicities in heavy and light quark initiated events above the Z0 peak*, Phys. Lett. **B550** (2002) 33, `arXiv:hep-ex/0211007`.